Journal of Zhejiang University-SCIENCE C (Computers & Electronics)
ISSN 1869-1951 (Print); ISSN 1869-196X (Online)
www.zju.edu.cn/jzus; www.springerlink.com
E-mail: jzus@zju.edu.cn

Dust collector localization in trouble of moving freight car detection system*

Fu-qiang ZHOU†, Rong ZOU, He GAO

(*School of Instrumentation Science and Optoelectronics Engineering, Beihang University, Beijing 100191, China*)

†E-mail: zfq@buaa.edu.cn

Received July 16, 2012; Revision accepted Dec. 20, 2012; Crosschecked Jan. 9, 2013

Abstract: For a long time, trouble detection and maintenance of freight cars have been completed manually by inspectors. To realize the transition from manual to computer-based detection and maintenance, we focus on dust collector localization under complex conditions in the trouble of moving freight car detection system. Using mid-level features which are also named flexible edge arrangement (FEA) features, we first build the edge-based 2D model of the dust collectors, and then match target objects by a weighted Hausdorff distance method. The difference is that the constructed weighting function is generated by the FEA features other than specified subjectively, which can truly reflect the most basic property regions of the 3D object. Experimental results indicate that the proposed algorithm has better robustness to variable lighting, different viewing angle, and complex texture, and it shows a stronger adaptive performance. The localization correct rate of the target object is over 90%, which completely meets the need of practical applications.

Key words: Hausdorff distance, Weighting function, Trouble detection, Rail transportation
doi:10.1631/jzus.C1200223 **Document code:** A **CLC number:** TP39; U279.3

1 Introduction

1.1 Overview and motivation

For a long time, trouble detection and maintenance of freight cars have been accomplished manually by inspectors. The quality of detection and maintenance was seriously limited by many factors, such as the weather and the subjective factors of inspectors. Gradually, the traditional detection method has become unsuitable for security checking of high-speed, heavy and large density run of trains. The trouble of moving freight car detection system (TFDS) (Liu and Wang, 2005) greatly enhances the efficiency and reliability of trouble detection. In the development of the TFDS system, automatic trouble recognition plays an important role, which promotes the transition of work from manual operation to computerized automatic recognition, and shows a great significance in railway safety.

Visual detection in TFDS is as illustrated in Fig. 1, where C0 to C10 are magnet triggered sensor groups. Dynamic images are captured by high-speed cameras, and then transmitted to control rooms by special optical fiber networks and analyzed. The trouble detection is achieved by combining human recognition with computerized automatic recognition. Fig. 2 shows the front-end image capturing equipment that takes pictures of key parts of freight cars. In this context, the localization of the 3D object called 'dust collectors' is investigated as shown in Fig. 3, and the requirements are as follows:

1. A dust collector is a rigid 3D object, and different views of the 3D object are shown in dynamic images owing to the high-speed motion of freight cars. The approach should not rely on a specific view of the object, and can detect instances of dust collectors from multiple views.

* Project supported by the National Natural Science Foundation of China (No. 61072134) and the Research Fund for the Doctoral Program of Higher Education of China (No. 20101102110033)
© Zhejiang University and Springer-Verlag Berlin Heidelberg 2013

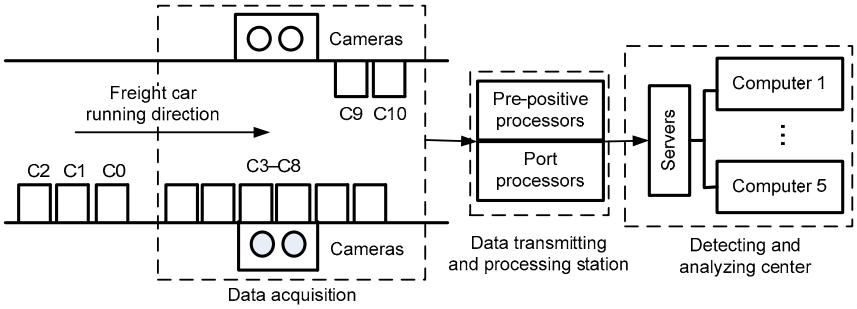

Fig. 1 Sketch of the trouble of moving freight car detection system (TFDS)

Fig. 2 Dynamic image capturing

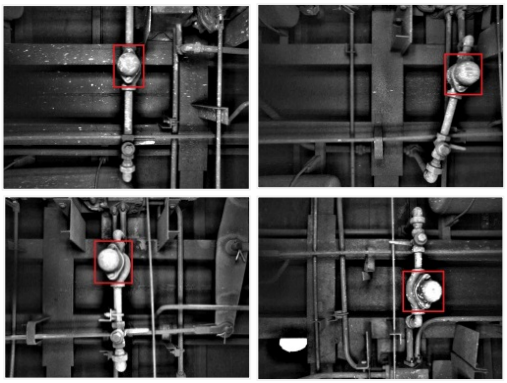

Fig. 3 Localizations of dust collectors

2. Texture changes on the dust collector surface due to wear and tear, surface scratches, and paint loss require non-appearance features to reliably detect the instances.

3. Because image capturing equipment is installed outdoors, the proposed algorithm should adequately take into account dust collector recognition under various illuminations, so as to localize the instances of dust collectors accurately.

1.2 Related works

With the development of visual detection technology, many visual trouble detection systems have emerged. A visual trouble detection system developed by Marino *et al.* (2007) is used to automatically detect the absence of the fastening bolts that secure the rails to the sleepers. The images of the rail are first obtained by a line scan camera, and then the real-time wavelet transform is applied for the extraction of features. The converted data are input into a multilayer perceptron neural network to achieve classification and identification. Zhang *et al.* (2011) used a structure light system and proposed a method based on dynamic structure light images to inspect missing fastening components in high-speed railway. Artificial neural networks are also used to recognize the absence of the fastening components. Yella *et al.* (2009) acquired sleeper images through a visual system and used the support vector machine (SVM) classifier to classify the sleeper images. They achieved a classification accuracy of 90%. de Ruvo *et al.* (2009) presented a graphics processing unit (GPU) based vision system to recognize rail fastening elements performing approximately 287% faster than a quad core CPU implementation. Hart *et al.* (2008) proposed a multi-spectral visual trouble detection system, which could detect the disc brake condition and the bearing performance. So far as we know, there has been no literature on dust collector localization.

In consideration of the object recognition technology requirements for dust collector localization, we divide object recognition into two categories: rigid and non-rigid. Rigid target recognition finds only the best pose parameters (Li and Hartley, 2007; Hartley and Kahl, 2009; Olsson *et al.*, 2009), which is relatively mature now. In recent years, non-rigid target recognition has been an important research field of computer vision. According to model formulations, it can also be divided into two categories: statistical and non-statistical model-based object recognition. An elastic template proposed by Grenander (1970) is a typical statistical model based method, and the template is generated by a characteristic generator and a

series of specific constraints, which adequately describe the variability of object instances. The method obtains a statistical model of an object through deformable templates. The statistical model of the image data and the prior are combined to define a posterior distribution on deformations given the image data. In subsequent work (Suk and Lee, 2013), a lot of theories were presented and applied to non-rigid object recognition in biological and medical fields. However, in practical applications, an elastic template needs to be initialized; i.e., some basic pose parameters must be set. In addition, the construction of a deformable template depends on a large number of elastic constraints among the characteristics (Amit *et al*., 1991; Amit, 1994; Zhu and Yuille, 1996; Chesnaud *et al*., 1999). Object recognition is achieved by maximizing the posterior distribution function. However, the deformation space is a multi-dimensional space, and there is still a very high computational cost even when pose parameters are known. The Bayesian model and Bernoulli model are often used in elastic template frameworks (Amit, 2002). Meanwhile, non-statistical models have been suggested by some researchers, such as an active contour model proposed by Kass *et al.* (1988), which is associated with the energy function defined properly, and minimized to the extraction of significant features. Bajcsy and Kovacic (1989) considered object deformation as image sequence analysis. Metaxas *et al.* (1997) first extracted feature points in the image, and then fitted the feature points to match curves or surfaces. This method shows the best performance only if the fitted curves or surfaces are smooth (Szeliski and Lavallée, 1996); however, curve or surface fitting is very difficult for complex shapes. The advantages of the method are that curve matching is easier than point matching. Chui and Rangarajan (2000) presented a non-rigid point matching algorithm based on a thin-plate spline function, which minimizes the bending energy of the thin-plate spline function to obtain a joint solution of matching matrix and mapping parameters under one-to-one corresponding constraints between point sets. These models use constraints instead of statistical models and their prior distributions, and the object deformation is evaluated by the cost function. The advantages of these non-rigid models are their strong adaptability, which has recently been introduced into 3D object recognition. It is suggested that 3D object recognition under different viewing angles should be treated as 2D non-rigid object recognition (Riesenhuber and Poggio, 2000) and a 2D model should be built. The 2D model should have some flexibility, which embodies a range of view angles instead of the establishment of a 3D model library. The current work is partially inspired by Riesenhuber and Poggio (2000).

In this paper, the problem of dust collector localization under complex conditions is researched. Due to the high-speed motion of a freight car and the fixed location of the image capturing equipment, the instances of dust collectors in the captured images significantly change in the viewing angle. In addition, to different types of freight cars, as well as to different parts of the same freight car, the locations and poses of dust collectors are also different (Fig. 3). We view the different poses and perspectives of the 3D target objects as a flexibility of 2D non-rigid objects. Furthermore, dust collectors are slightly different in size and shape, which is viewed as another flexibility of 2D non-rigid objects. Based on the above two kinds of flexibilities, flexible edge arrangement (FEA) features are used to build an edge-based 2D model of a dust collector. We propose a novel weighted Hausdorff distance for dust collector localization under complex conditions. The Hausdorff distance is an effective similarity measure for binary image comparison, and introduction of a weighting function improves the robustness of Hausdorff distance matching. Our algorithm solves the problem of dust collector localization under variable lighting, changes in the viewing angle, and variable textures. Our contribution is that the weighting function is built using FEA features. According to the frequency of each feature, the generated weighting function highlights the key features, which greatly improves the accuracy of Hausdorff distance matching and establishes a foundation for the following trouble detection.

2 Proposed algorithm

Using FEA features, we first build an edge-based 2D model and a corresponding weighting function, and localize dust collectors by the new weighted Hausdorff distance. Different from low-level features, FEA features are mid-level features, which are

constructed not through hand-coding but through training. They capture all the important information that is useful for recognizing target objects.

2.1 Edge-based 2D model

In this section, the first stage of our approach will be described. We take the view-based approach in which different views of dust collectors are to be considered as different 2D objects that are linked together symbolically. The problem then is simplified for the recognition of a non-rigid 2D object. Given images of the 3D objects under different views, we wish to generate an edge-based 2D model.

2.1.1 FEA features

Each FEA feature (Amit, 2002) is defined in terms of a 'central edge' of some type e_0, and a number n_r of other edge types e_1, e_2, …, e_r, which are correspondingly constrained in specific subregions R_1, R_2, …, R_{n_r}, in the neighborhood of the location of the center edge. We refer to the number n_r of additional edges as complexity of FEA features, and an FEA feature with n_r=4 is shown in Fig. 4, which includes a central edge e_0, and edges e_1, e_2, e_3, and e_4 in four subregions R_1, R_2, R_3, and R_4, respectively.

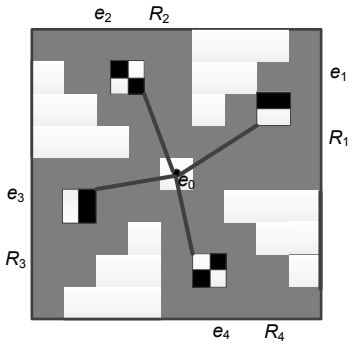

Fig. 4 A flexible edge arrangement (FEA) feature with n_r=4

2.1.2 2D model construction

FEA features are detected at a location if an instance of e_0 is found at that location and instances of n_r additional edges are found in the corresponding region. The family of possible subregions is denoted by $\boldsymbol{\Phi}$. The sizes of the subregions are all approximately the same, and their shape is wedge-shaped in the neighborhood of the center (Fig. 5). When the complexity of FEA features is higher (i.e., n_r>1), the number of possible arrangements is very large. A greedy search is implemented instead to seek stepwise increments in the complexity of features with a high frequency on the object class. Edges are first detected on each training image and their locations are registered to the reference grid using the affine map $\boldsymbol{A}_p$. In each disjoint $c\times c$ box of the reference grid, the n_r=2 FEA features with the highest count are first found. All instances of the FEA features in the box are recorded for each image. Then, a loop over all possible additions of one edge pair selects the one with the highest count in the box, until the desired complexity n_r edge pairs are found. More explicitly, we provide a summary of the training procedure as follows:

Input:
Complexity n_r.
Feature occurrence probability ρ.
Family of wedge-shaped subregions $\boldsymbol{\Phi}$.
Training set $\boldsymbol{\Omega}$.
Output:
FEA feature map.
Initialization:
Set feature counter i=0.
Algorithm:
1. Detect edges in all training images $\boldsymbol{\Omega}$.
2. Register edge maps into a reference grid.
3. Loop over disjoint $c\times c$ (c=3 or 5) boxes on the reference grid.
4. For each such box $\boldsymbol{C}$:
(a) For each possible combination (e, e', R), where e, e' are some type edges and $R\in\boldsymbol{\Phi}$, count the number of training images for which e, the central edge, is at some $x\in\boldsymbol{C}$ and $e'\in x+R$.
(e_0, e_1, R_1)—combination with the highest count.
$\boldsymbol{\Omega}_1$—training images with an instance of (e_0, e_1, R_1) in $\boldsymbol{C}$.
For $d\in\boldsymbol{\Omega}_1$, $x_{d,t}\in\boldsymbol{C}$, t=1, 2, …, $n_{d,t}$, locations of e_0 for which combination was found. Set j=2.
(b) For each possible combination (e, R), count the number of data images $d\in\boldsymbol{\Omega}_{j-1}$ for which there is an edge $e\in x_{d,t}+R$, for some t=1, 2, …, $n_{d,j-1}$.
(e_j, R_j)—combination with the highest count.
$\boldsymbol{\Omega}_j\subset\boldsymbol{\Omega}_{j-1}$—training images that have an instance of the combination (e_j, R_j).
For $d\in\boldsymbol{\Omega}_j$, $x_{d,t}$, t=1, 2, …, $n_{d,j}$ instances of e_0 for which (e_j, R_j) was found.
(c) $j\leftarrow j$+1. If $j<n_r$ goto (b).
5. If $|\boldsymbol{\Omega}_{n_r}|/|\boldsymbol{\Omega}|>\rho$, record the feature
$\boldsymbol{X}_i$=(e_0, e_1, R_1, …, e_{n_r}, R_{n_r}) at z_i—center of $\boldsymbol{C}$.
All images in $\boldsymbol{\Omega}_{n_r}$ have an instance of e_0 at some $x\in\boldsymbol{C}$ and an instance of e_k in $x+R_k$, for each k=1, 2, …, n_r.
6. Move to the next box $i\leftarrow i$+1, goto 3.

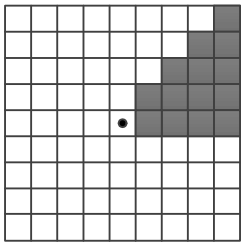

Fig. 5 Wedge-shaped subregions

Fig. 6b shows the final generated FEA feature map of a dust collector shown in Fig. 6a. Some training examples are shown in Fig. 7. We use 62 sample images for training. To balance computational complexity and recognition performance, we adopt the FEA features with the complexity n_r=3 (Fig. 6c).

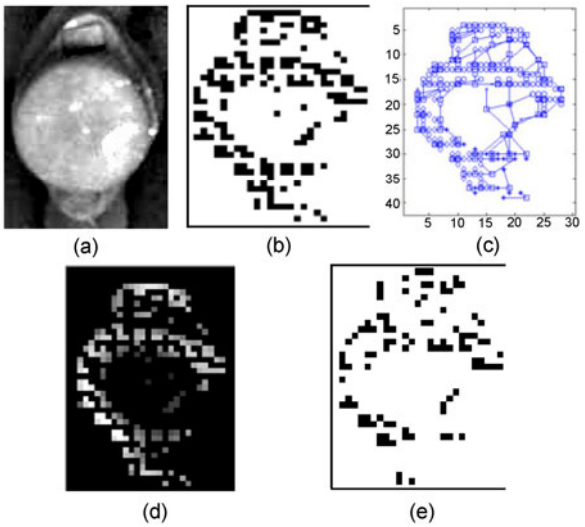

Fig. 6 Edge-based 2D model and weighting function
(a) Rototype image; (b) FEA feature map; (c) FEA feature structure; (d) Weighting function; (e) Sparse template

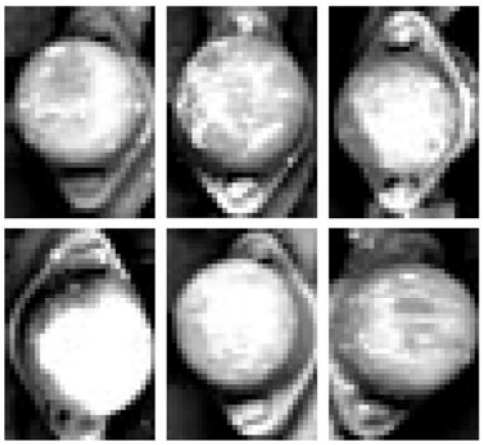

Fig. 7 Training examples

2.2 Weighted Hausdorff distance matching

3D object recognition under very different lighting conditions is a very challenging problem, and requires a robust image matching algorithm. The Hausdorff distance and its variants have been recognized to provide an effective way for image matching mainly because feature correspondence is not required.

2.2.1 Conventional Hausdorff distance

For two finite point sets $A=\{\boldsymbol{a}_1, \boldsymbol{a}_2, \ldots, \boldsymbol{a}_p\}$ and $B=\{\boldsymbol{b}_1, \boldsymbol{b}_2, \ldots, \boldsymbol{b}_q\}$, the conventional Hausdorff distance (Shi *et al*., 2009) is defined as

$$H(A, B)=\max\big(h(A, B), h(B, A)\big), \qquad (1)$$

where $h(A,B)=\max\limits_{\boldsymbol{a}\in A}\min\limits_{\boldsymbol{b}\in B}\|\boldsymbol{a}-\boldsymbol{b}\|$, and $\|\boldsymbol{a}-\boldsymbol{b}\|$ is the Euclidean distance between $\boldsymbol{a}$ and $\boldsymbol{b}$. The function $h(A, B)$ is called the forward Hausdorff distance from A to B. It represents the point $\boldsymbol{a}\in A$ that is farthest from any point of B and measures the distance from $\boldsymbol{a}$ to its nearest neighbor in B (using the given norm $\|\cdot\|$); that is, $h(A, B)$ in effect ranks each point of A based on its distance to the nearest point of B, and then uses the largest ranked point as the distance (the most mismatched point of A). The reversed Hausdorff distance $h(B, A)$ can be represented similarly. The Hausdorff distance $H(A, B)$ is the maximum between $h(A, B)$ and $h(B, A)$.

2.2.2 Weighted Hausdorff distance

The robustness of the conventional Hausdorff distance measure is very poor. Many improvements have been proposed to obtain a more reliable and more robust distance measure. Dubuisson and Jain (1994) proposed a modified Hausdorff distance (MHD) measure as the object matching metric. Jesorsky *et al*. (2001) used MHD to localize face position. The directed MHD is defined as

$$h(A, B)=\frac{1}{N_{\boldsymbol{a}}}\sum_{\boldsymbol{a}\in A}\min_{\boldsymbol{b}\in B}\|\boldsymbol{a}-\boldsymbol{b}\|, \qquad (2)$$

where $N_{\boldsymbol{a}}$ is the number of points in A. Lin *et al*. (2003) proposed the spatially weighted Hausdorff distance (SWHD) and spatially eigen-weighted Hausdorff distance (SEWHD) to reflect the importance of

different regions in the human face. Both the same form of the two Hausdorff distances and the directed Hausdorff distance are expressed as

$$h(A,B)=\frac{1}{N_{\boldsymbol{a}}}\sum_{\boldsymbol{a}\in A}w(\boldsymbol{b})\min_{\boldsymbol{b}\in B}\|\boldsymbol{a}-\boldsymbol{b}\|, \tag{3}$$

where $w(\boldsymbol{b})$ is the weighting function. For SWHD, the weighting function is manually specified according to the space information of faces, and SEWHD generates the weighting function by the first eigenface of the training set. Tan and Zhang (2006) proposed to weight on the common area of faces. The weighting function embodies the common features of objects, which is introduced to Hausdorff distance metrics, and can significantly improve matching accuracy and robustness. However, a critical issue is how to build the weighting function. Face images have an intuitive view that the eyes, mouth, and face contour are the most common properties, and in these areas the pixels should have greater weights. For general 3D objects with little or no texture, it is more difficult to reasonably and non-subjectively reflect the most crucial features of the 3D objects under different views and illumination variations. Generating the weighting function through FEA features is a good solution to this problem.

2.2.3 Generating weighting function

We generate a weighting function through FEA features, and the weight is obtained by the relative frequency of each feature in the training. That is,

$$w(x,y)=\frac{1}{N}\sum_{i\in N}F_i(x,y), \tag{4}$$

where $F_i(x, y)$ is the FEA feature of the ith training image in the position (x, y), and N is the total number of images in the training set. The weighting function generated of a dust collector is shown in Fig. 6d. The new weighted Hausdorff distance is called the flexible weighted Hausdorff distance (FWHD).

2.2.4 FEA feature model matching

Let the 2D point sets A and B denote the tested edge image and the 2D FEA feature model of the 3D object, respectively. The goal of matching is to find the transformation parameter p, such that the Hausdorff distance between the transformed model $T_p(B)$ and A is minimized, which is expressed as

$$d=\min_{p\in\boldsymbol{P}}H\left(A,T_p(B)\right). \tag{5}$$

Allowed transformations (scale, rotation, and translation), namely the parameter space $\boldsymbol{P}$, depend on the specific practical application. Since the space $\boldsymbol{P}$ of affine transformations from the model shape is large, an efficient matching scheme was introduced by Rucklidge (1997), which examines only a small part of the space of the affine transformations. In practice, we adopt the method suggested by Rucklidge (1997). The transformation space $\boldsymbol{P}$ is discretized to approximate the search for the exact minimizing transformation. The flowchart of the algorithm of dust collector localization is shown in Fig. 8. Note that a sliding window based method is used to locate a dust collector. Each image is densely scanned from the top left to the bottom right with rectangular sliding windows. We search all windows of the image with dimensions $u\times v$, which may represent the template B in the $m\times n$ dimension image to find which window has the minimum distance to the template. In experiments, the size of the image is 260×194 and that of the template is 30×42.

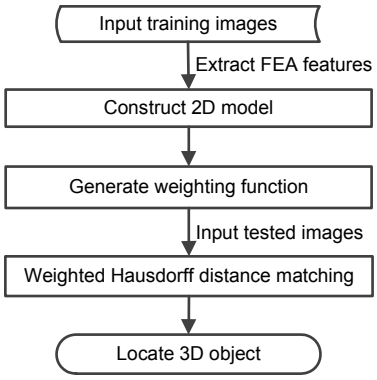

Fig. 8 Flowchart of the proposed algorithm

3 Experimental results and analysis

To test the effectiveness of the algorithm, we apply the proposed method to localize dust collectors with various viewing angles in real images. Considering that the FEA features are mid-level features,

the structure of the model can be relatively simple, without using all the FEA features. In this study, we randomly select the FEA features to generate a sparse model template, which reduces the computational cost. For dust collectors, the algorithm extracts a total of 78 FEA features, and randomly selects 40 FEA features to build sparse models (Fig. 6e). The FEA features reflect the most essential common features of the 3D object, which makes it possible to overcome the disadvantageous effects of viewing angle changes by combining the FEA features with the weighting function, and exactly match the target object. Fig. 9 shows the localization results of the experiments under different views.

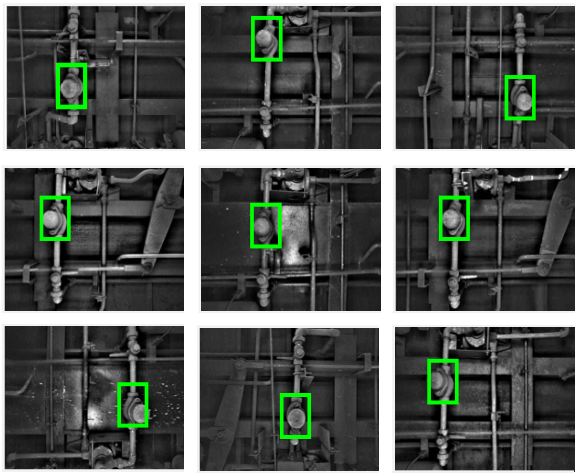

Fig. 9 Localization results under different views

Fig. 10 shows the test results under texture changes. The algorithm can still accurately localize the dust collectors, which is immune to a variety of bright spot distribution. The reason is that FEA features are mid-level features with complex structures. Mid-level features have a relatively good discrimination performance, and a weighting function generated by the mid-level features strengthens its anti-noise performance. The results show that our algorithm can accomplish dust collector localization in complex conditions.

In addition, FEA features are contour features, which are robust to direction changes of illumination. Moreover, the weighting function can effectively suppress fake contours generated by illumination variations, and enhance the real contour, which ensures reliable localization. Fig. 11 shows the localization results of our algorithm under different illumination directions.

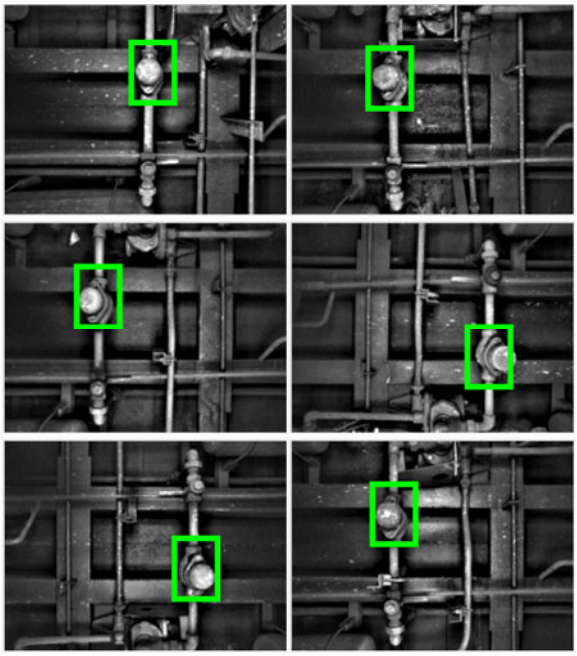

Fig. 10 Localization results under texture changes

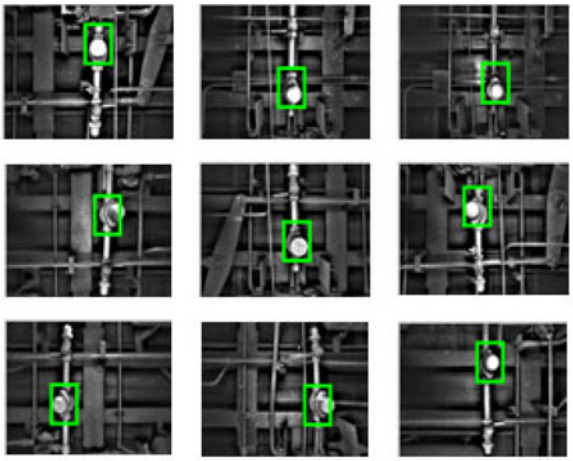

Fig. 11 Localization results under different illumination directions

To further test the performance of the proposed algorithm, we obtain image samples in three different sites to create three image databases. Since the purpose of our algorithm is to localize the dust collectors exactly, what we primarily care about is the correctness of dust collector localization in this experiment. We randomly select more than 200 real image samples from each database, which is referred to as dataset D1, D2, or D3, and test the localization performance of our algorithm. We carry out the experiment under the PC condition of Intel Pentium 4 CPU 3.00 GHz, memory 1 GB, Win7 OS, and the

MATLAB 2009b programming environment. Its time consumption is 384 ms for a 260×194 image. The localization results are summarized in Table 1. Note that the proposed algorithm has good localization performance, which completely meets the need of practical applications.The fault localization images are shown in Fig. 12. They are mainly due to too large inclination angles and extreme overexposure. With respect to a few images under uneven lighting, errors are sometimes generated by the algorithm.

The matching accuracy of our algorithm is also tested. We select 27 real image samples that can be correctly localized by two measures, including FWHD and MHD, and calculate the distances between our 2D model and testing images. The normalized matching distance errors are shown in Fig. 13. From the experimental results, the proposed FWHD can localize the dust collectors in the image more accurately than others.

Table 1 Localization results in three image datasets

Dataset	Image number	Correct number	Fault number	Correct rate (%)
D1	206	189	17	91.7
D2	202	183	19	90.6
D3	207	189	18	91.3

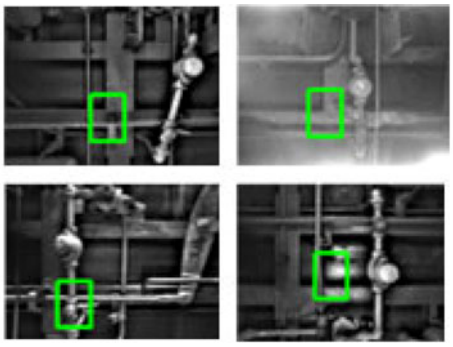

Fig. 12 Images of fault localizations

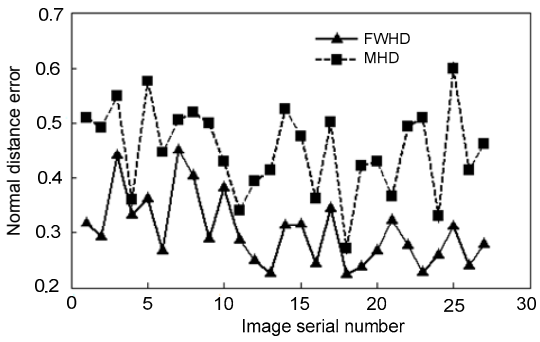

Fig. 13 Verification results of matching accuracy

4 Conclusions

The inspection of key parts of freight cars is very important for railway safety. In this paper, we focus on the localization of dust collectors under complex conditions. We first construct a 2D FEA feature model of dust collectors, and apply the weighted Hausdorff distance measure to match the 3D target objects, which achieves accurate localizations of the dust collectors. In the matching process, the weighting function is introduced to improve the robustness and localization accuracy of the algorithm. Experimental results have proved the effectiveness of our algorithm. Our contributions are:

1. Introduce 2D recognition ideas for a 3D object and use FEA features to generate a 2D model, only by applying a template to the localization of the dust collectors.

2. Propose the idea of using FEA features to build the weighting function, and effectively express the common properties of the general 3D object with different views.

3. Combine the FEA features with a weighting function to successfully resolve the problems of different illumination and texture changes, which expands the application.

In short, the proposed algorithm based on a single template has low computational complexity and immunity to noise. It has strong adaptability to poor quality images.

References

Amit, Y., 1994. A nonlinear variational problem for image matching. *SIAM J. Sci. Comput.*, **15**(1):207-224. [doi:10.1137/0915014]

Amit, Y., 2002. Sparse Models: Formulation, Training, and Statistical Properties. The MIT Press, Cambridge, US, p.121-137.

Amit, Y., Grenander, U., Piccioni, M., 1991. Structural image restoration through deformable templates. *J. Am. Stat. Assoc.*, **86**(414):376-387. [doi:10.1080/01621459.1991.10475053]

Bajcsy, R., Kovacic, S., 1989. Multiresolution elastic matching. *Comput. Vis. Graph. Image Process.*, **46**(1):1-21. [doi:10.1016/S0734-189X(89)80014-3]

Chesnaud, C., Réfrégier, P., Boulet, V., 1999. Statistical region snake-based segmentation adapted to different physical noise models. *IEEE Trans. Pattern Anal. Mach. Intell.*, **21**(11):1145-1157. [doi:10.1109/34.809108]

Chui, H., Rangarajan, A., 2000. A New Algorithm for Non-rigid Point Matching. IEEE Conf. on Computer Vision and Pattern Recognition, p.44-51. [doi:10.1109/

CVPR.2000.854733]

de Ruvo, P., Distante, A., Stella, E., Marino, F., 2009. A GPU-Based Vision System for Real Time Detection of Fastening Elements in Railway Inspection. IEEE Int. Conf. on Image Processing, p.2333-2336. [doi:10.1109/ICIP.2009.5414438]

Dubuisson, M.P., Jain, A.K., 1994. A Modified Hausdorff Distance for Object Matching. Proc. 12th Int. Conf. on Pattern Recognition, p.566-568. [doi:10.1109/ICPR.1994.576361]

Grenander, U., 1970. A unified approach to pattern analysis. *Adv. Comput.*, **10**(1):175-216. [doi:10.1016/S0065-2458(08)60436-2]

Hart, J.M., Resendiz, E., Freid, B., Sawadisavi, S., Barkan, C., Ahuja, N., 2008. Machine Vision Using Multi-spectral Imaging for Undercarriage Inspection of Railroad Equipment. Proc. 8th World Congress on Railway Research, p.1-8.

Hartley, R.I., Kahl, F., 2009. Global optimization through rotation space search. *Int. J. Comput. Vis.*, **82**(1):64-79. [doi:10.1007/s11263-008-0186-9]

Jesorsky, O., Kirchberg, K., Frischholz, R.W., 2001. Robust face detection using the Hausdorff distance. *LNCS*, **2091**: 90-95. [doi:10.1007/3-540-45344-x_14]

Kass, M., Witkin, A., Terzopoulos, D., 1988. Snakes: active contour models. *Int. J. Comput. Vis.*, **1**(4):321-331. [doi:10.1007/BF00133570]

Li, H., Hartley, R., 2007. The 3D-3D Registration Problem Revisited. IEEE 11th Int. Conf. on Computer Vision, p.1-8. [doi:10.1109/ICCV.2007.4409077]

Lin, K.H., Lam, K.M., Siu, W.C., 2003. Spatially eigen-weighted Hausdorff distances for human face recognition. *Pattern Recogn.*, **36**(8):1827-1834. [doi:10.1016/S0031-3203(03)00011-6]

Liu, R., Wang, Y., 2005. Principle and Application of TFDS. China Railway Publication, Beijing, p.1-20 (in Chinese).

Marino, F., Distante, A., Mazzeo, P.L., Stella, E., 2007. A real-time visual inspection system for railway maintenance: automatic hexagonal-headed bolts detection. *IEEE Trans. Syst. Man. Cybern. Part C Appl. Rev.*, **37**(3): 418-428. [doi:10.1109/TSMCC.2007.893278]

Metaxas, D., Koh, E., Badler, N.I., 1997. Multi-level shape representation using global deformations and locally adaptive finite elements. *Int. J. Comput. Vis.*, **25**(1):49-61. [doi:10.1023/A1007929702347]

Olsson, C., Kahl, F., Oskarsson, M., 2009. Branch-and-bound methods for Euclidean registration problems. *IEEE Trans. Pattern Anal. Mach. Intell.*, **31**(5):783-794. [doi:10.1109/TPAMI.2008.131]

Riesenhuber, M., Poggio, T., 2000. Models of object recognition. *Nat. Neurosci.*, **3**:1199-1204. [doi:10.1038/81479]

Rucklidge, W.J., 1997. Efficiently locating objects using the Hausdorff distance. *Int. J. Comput. Vis.*, **24**(3):251-270. [doi:10.1023/A:1007975324482]

Shi, F., Yang, J., Zhu, Y., 2009. Automatic segmentation of bladder in CT images. *J. Zhejiang Univ.-Sci. A*, **10**(2): 239-246. [doi:10.1631/jzus.A0820157]

Suk, H., Lee, S., 2013. A novel Bayesian framework for discriminative feature extraction in brain-computer interfaces. *IEEE Trans. Pattern Anal. Mach. Intell.*, **35**(2): 286-299. [doi:10.1109/TPAMI.2012.69]

Szeliski, R., Lavallée, S., 1996. Matching 3-D anatomical surfaces with non-rigid deformations using octree-splines. *Int. J. Comput. Vis.*, **18**(2):171-186. [doi:10.1007/BF00055001]

Tan, H., Zhang, Y.J., 2006. A novel weighted Hausdorff distance for face localization. *Image Vis. Comput.*, **24**(7): 656-662. [doi:10.1016/j.imavis.2005.05.011]

Yella, S., Dougherty, M., Gupta, N.K., 2009. Condition monitoring of wooden railway sleepers. *Transp. Res. Part C Emerg. Technol.*, **17**(1):38-55. [doi:10.1016/j.trc.2008.06.002]

Zhang, H., Yang, J., Tao, W., Zhao, H., 2011. Vision method of inspecting missing fastening components in high-speed railway. *Appl. Opt.*, **50**(20):3658-3665. [doi:10.1364/AO.50.003658]

Zhu, S.C., Yuille, A., 1996. Region competition: unifying snakes, region growing, and Bayes/MDL for multiband image segmentation. *IEEE Trans. Pattern Anal. Mach. Intell.*, **18**(9):884-900. [doi:10.1109/34.537343]